

AD-A258 709

2

PL-TR-91-2290 (I)

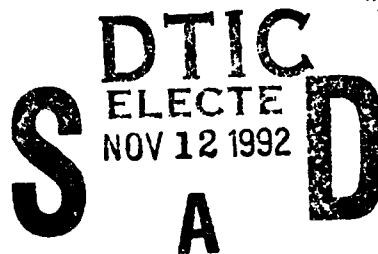


**Design Recommendations For The Smart Weapons Operability
Enhancement Three-Dimensional Thermal Model**

J. R. Hummel
M.G. Cheifetz

SPARTA, Inc.
24 Hartwell Avenue
Lexington, MA 02173

26 November 1991



Final Report Volume I
September 1990 - March 1991

Approved for Public Release; Distribution Unlimited

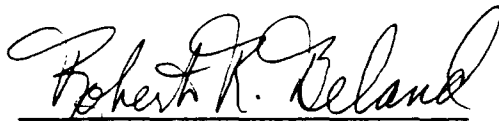


PHILLIPS LABORATORY
AIR FORCE SYSTEMS COMMAND
HANSCOM AIR FORCE BASE, MASSACHUSETTS 01731-5000

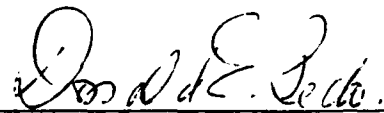
92-29308



"This technical report has been reviewed and is approved for publication"



ROBERT R. BELAND
CONTRACT MANAGER



DONALD E. BEDO
BRANCH CHIEF



ALAN D. BLACKBURN, Col., USAF
DIVISION DIRECTOR

This report has been reviewed by the ESD Public Affairs Office (PA) and is releasable to the National Technical Information Service (NTIS).

Qualified requestors may obtain additional copies from the Defense Technical Information Center. All others should apply to the National Technical Information Service.

If your address has changed, or if you wish to be removed from the mailing list, or if the addressee is no longer employed by your organization, please notify PL/IMA, Hanscom AFB, MA 01731-5000. This will assist us in maintaining a current mailing list.

Do not return copies of this report unless contractual obligations or notices on a specific document requires that it be returned.

REPORT DOCUMENTATION PAGE			Form Approved OMB No. 0704-0188	
Public reporting burden for this collection of information is estimated to average 1 hour per response, including the time for reviewing instructions, searching existing data sources, gathering and maintaining the data needed, and completing and reviewing the collection of information. Send comments regarding this burden estimate or any other aspect of this collection of information, including suggestions for reducing this burden, to Washington Headquarters Services, Directorate for Information Operations and Reports, 1215 Jefferson Davis Highway, Suite 1204, Arlington, VA 22202-4302, and to the Office of Management and Budget, Paperwork Reduction Project (0704-0188), Washington, DC 20503.				
1. AGENCY USE ONLY (Leave blank)		2. REPORT DATE 26 November 1991		3. REPORT TYPE AND DATES COVERED Sep 90 - 3 Mar 91, Final Report, Volume I
4. TITLE AND SUBTITLE Design Recommendations for the Smart Weapons Operability Enhancement Three-Dimensional Thermal Model			5. FUNDING NUMBERS PE 62101F PR 7670TA15WUAP Contract- F19628-88-C-0038	
6. AUTHOR(S) J. R. Hummel and M. G. Cheifetz				
7. PERFORMING ORGANIZATION NAME(S) AND ADDRESS(ES) SPARTA, Inc. 24 Hartwell Avenue Lexington, MA 02173			8. PERFORMING ORGANIZATION REPORT NUMBER LTR91-017	
9. SPONSORING / MONITORING AGENCY NAME(S) AND ADDRESS(ES) PHILLIPS LABORATORY HANSCOM AIR FORCE BASE, MASSACHUSETTS 01731-5000 Contract Manager: Robert Beland/GPOA			10. SPONSORING / MONITORING AGENCY REPORT NUMBER PL-TR-91-2290 (I)	
11. SUPPLEMENTARY NOTES				
12a. DISTRIBUTION / AVAILABILITY STATEMENT Approved for Public Release; Distribution Unlimited			12b. DISTRIBUTION CODE	
13. ABSTRACT (Maximum 200 words) The modeling and understanding of the radiant structure from natural backgrounds is a complex undertaking due to the great variability in scene elements. The physical processes describing the radiant field, as well as many of the objects generating the radiation, are three dimensional (3-D) in nature so a full 3-D treatment of the physics is necessary in order to properly describe the radiant field. However, the theoretical requirement for a 3-D treatment of the physics must be balanced against the practical realities of what 3-D processes are actually important and if proper and complete data resources are available to justify the detailed calculations. This report presents results from a study designed to establish design recommendations for a multi-dimensional energy balance model. Results will be presented to detail under what conditions a multi-dimensional treatment of the energy balance for natural backgrounds must be performed and under what conditions 1-D calculations are sufficient.				
14. SUBJECT TERMS BTI/SWOE, 3-D Thermal models			15. NUMBER OF PAGES 44	
			16. PRICE CODE	
17. SECURITY CLASSIFICATION OF REPORT UNCLASSIFIED	18. SECURITY CLASSIFICATION OF THIS PAGE UNCLASSIFIED	19. SECURITY CLASSIFICATION OF ABSTRACT UNCLASSIFIED	20. LIMITATION OF ABSTRACT SAR	

Accession For	
NTIS CRA&I	<input checked="" type="checkbox"/>
DTIC TAB	<input type="checkbox"/>
Unannounced	<input type="checkbox"/>
Justification	
By	
Distribution /	
Availability Codes	
Dist	Avail and/or Special
A-1	

DTIC QUALITY INSPECTED 4

Contents

1	INTRODUCTION	1
1.1	Background and Purpose of Research	1
1.2	Organization of Report	4
2	GENERAL MODELING APPROACH	4
2.1	Required Capabilities for a SWOE Test Bed Code	5
2.2	Recommended Numerical Experiments	5
3	BOUNDARIES BETWEEN DIFFERENT MATERIALS	7
3.1	One-Dimensional Thermal Calculations	8
3.1.1	Convective Cooling	9
3.1.2	Discussion of Results	10
3.2	Two-Dimensional Thermal Boundary Model Calculations	13
3.2.1	Discussion of Results	13
3.2.2	Sensitivity of Thermal Field to Buried Rock Width	16
4	THREE DIMENSIONAL OBJECTS EMBEDDED IN THE SCENE	18
4.1	3-D Rock Embedded in Soil	19
4.2	3-D Rock Placed On Top of Soil	20
5	INHOMOGENEOUS DISTRIBUTION OF MATERIALS	26
6	SUMMARY AND RECOMMENDATIONS	28
6.1	Summary	28
6.1.1	Boundaries Between Different Classes of Materials	30
6.1.2	Objects Embedded in Scenes	30
6.1.3	Inhomogeneous Distribution of Materials	31

6.2 Recommendations	31
6.2.1 Boundaries Between Different Materials	31
6.2.2 Presence of 3-D Scene Objects	31
6.2.3 Inhomogeneous Distribution of Materials	32
REFERENCES	33
APPENDIX A: Summary SPARTA's TRAC-3 3-D Thermal Response Code	34

Figures

1	Thermal Image of a Forest Edge With a Gap Exposing the Interior Portions of the Forest	3
2	Air Temperatures as a Function of Time at Hunfeld, Germany on 10 September 1982	6
3	Calculated Total Solar Fluxes as a Function of Time of Day at Hunfeld, Germany on 10 September 1982	6
4	Scene With Marked Boundaries Between Material Types	7
5	Schematic Representation of the Variable Grid Scheme Used for the 1-D Thermal Calculations	9
6	Calculated 1-D Sand and Granite Skin Temperatures as a Function of Time With and Without Convective Cooling Considered	11
7	Calculated 1-D Soil Skin Temperatures as a Function of Time With and Without Convective Cooling Considered	11
8	Calculated Skin Temperatures as a Function of Time for (a.) Granite, (b.) Sand, and (c.) Soil Type III Demonstrating the Importance of Convective Cooling	12
9	Grid Scheme Used for 2-D Calculations of a Buried Rock	14
10	2-D Skin Temperatures as a Function of Time for a Rock Embedded in (a.) Sand and (b.) Soil Type III	15
11	Temperatures at 1500 Hours Along a Line Passing Through a Granite Rock Embedded in Soil	17
12	Temperatures Along a Line Passing Through an Embedded Rock as a Function of Time of Day	17
13	Impact of Rock Width on 2-D Temperature Calculations	18
14	Complex Scene With Embedded 3-D Objects	19

15	Schematic Representation of the Buried Rock Model Used in the 3-D Calculations of a Rock in Soil	20
16	Position of Slices and Reference Points Used in the Buried Rock 3-D Thermal Calculations	21
17	Skin Temperatures as a Function of Time for Different Points on the Surface of a Rock Buried in Sand	22
18	Comparisons of Skin Temperatures as a Function of Time Near the Sand/Rock Interface and the Rock Interior for the 3-D Thermal Calculations of a Rock Buried in Sand	23
19	Schematic Representation of a Rock Placed On Top of Sand	24
20	Total Solar Fluxes Incident on the 3-D Rock Faces as a Function of Time of Day	25
21	Calculated Skin Temperatures as a Function of Time at Positions at the Midpoint of Different Rock Faces	25
22	Sketch of a Soil Cross Section With Uniform and Nonuniform Soil Stratification	26
23	Comparison of Soil Temperatures at Two Closely Spaced Locations at (a.) 1 cm and (b.) 20 cm Below the Surface	29

Tables

1	Thermal Properties of Soils and Rock Materials	8
2	Calculated Peak Temperatures With and Without Convective Cooling Effects and the Difference Between the Two Temperatures	13
3	Relative Importance of Surface Temperature to Changes in Material Properties	27

Design Recommendations for the Smart Weapons Operability Enhancement Three-Dimensional Thermal Model

1 INTRODUCTION

1.1 Background and Purpose of Research

The Balanced Technology Initiative (BTI) on Smart Weapons Operability Enhancement (SWOE) has as a goal to model the radiant field from complex natural backgrounds. Key to achieving this goal is a model of the thermal structure of the natural background. The physical processes controlling this thermal structure are three dimensional in nature so a full three dimensional treatment of the physics is necessary in order to properly and correctly describe the radiant field.

The development of a three dimensional thermal model of the natural background is a significant undertaking. As a first step in the development, a review of available one dimensional (1-D) thermal models was performed¹ for the BTI/SWOE

¹ Balick, L.K., Hummel, J.R., Smith, J.A., and Kimes, D.S. (1990) "One Dimensional Temperature Modeling Techniques for the BTI/SWOE: Review and Recommendations", SWOE Program Office, US Army Cold Regions Research and Engineering Laboratory, Hanover, NH, SWOE Report 90-1, August.

program and recommendations given on what models or modules could be used to serve as an interim thermal model (ITM) while the 3-D package was under development. The SWOE ITM has been developed² and is available to users while a full 3-D package is being developed.

The types of backgrounds that must be considered in the BTI/SWOE program include solid materials without vegetation, porous materials, surfaces with different levels of vegetation, snow and ice covered surfaces, and bodies of water, to name just a few. Modeling the dynamic thermal structure of these surfaces requires a detailed study of the energy and mass transfer through materials, as a result of either heat or mass transport. Although the type of material may change, the basic set of physical processes of energy transport remain the same. However, many situations require much more ambitious three dimensional representations of the energy transfer. An example of just such a situation is shown in Figure 1.

The figure displays an 8 - 12 μ m image of a forest edge with a gap present. The edge, by itself, is a three dimensional object with radiances being produced at different levels. With the gap present, the interior regions of the forest are exposed and contribute to the sensed radiant field. The three dimensionality of the problem becomes more apparent when the deciduous foliage is removed and more of the interior portions are exposed.

A first order review of scene simulation possibilities produces three situations where three dimensional thermal effects are important. They are:

1. Boundaries between different types of materials, such as dirt and concrete.
2. Objects which are embedded in the scene, such as buildings, boulders, individual trees, or vehicles.
3. Inhomogeneous distributions of materials such as rocky soil, sparse tree cover, or heavily tracked surfaces.

Since the nature of the substrate influences the energy balance, the effects of embedded objects and surface inhomogeneities may also appear in the substrate rather than only at the surface.

SPARTA has developed a three dimensional model, TREETHERM, of the thermal balance of individual trees.³ The model, has provided a framework for the

² Hummel, J.R., Jones, J.R., Longtin, D.R., and Paul, N.L. (1991) "Development of the Smart Weapons Operability Enhancement Interim Thermal Model", Phillips Laboratory, Hanscom AFB, Massachusetts, PL-TR-91-2073, March, ADA 238995.

³ Hummel, J.R., Jones, J.R., Longtin, D.R., and Paul, N.L. (1991) "Development of a 3-D Tree Thermal Response Model for Energy Budget and Scene Simulation Studies", Phillips Laboratory, Hanscom AFB, Massachusetts, PL-TR-91-2109, March, ADA 240509.

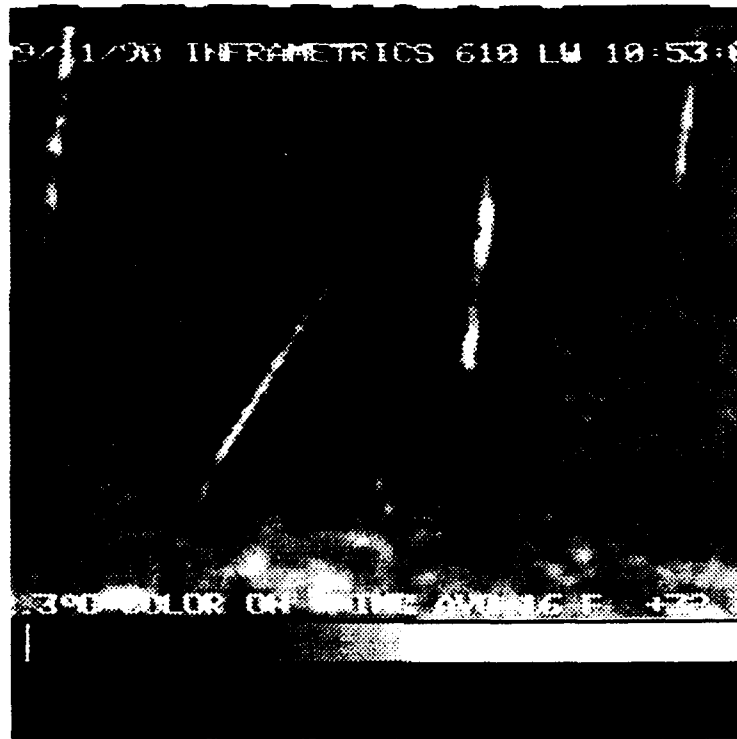


Figure 1. Thermal Image of a Forest Edge With a Gap Exposing the Interior Portions of the Forest

development of a 3-D thermal model for generalized objects which, when combined with the results from this study, will provide the development plan for the full SWOE 3-D thermal model.

Although the physical processes contributing to the thermal structure are the same in one dimensional and three dimensional representations, the added complexity of having energy transported in additional directions, and the inherent capacity for more spatial variability in materials and material properties, combine to make three dimensional models much more complex. Comprehensive three dimensional models should be developed only after the three dimensional aspects of the thermal balance have been demonstrated to be an important factor in the energy transport.

The purpose of this research was to advocate an approach for determining when multi-dimensional thermal modeling is required. This was performed by utilizing existing thermal modeling tools, such as a three dimensional thermal response code in use at SPARTA, (see the Appendix for a discussion of this model) as a test bed for establishing the importance of multi dimensional thermal effects.

1.2 Organization of Report

This report is divided into four main sections. Section 2 defines a general modeling approach for a SWOE simulation including the required capabilities for a SWOE multi-dimensional test bed model. Section 3 addresses the issue of boundaries between various types of backgrounds. Section 4 discusses the problem of 3-D objects embedded in a scene. Section 5 investigates the effect of inhomogeneous distributions of materials on the thermal field. Finally, Section 6 presents a summary of the study and recommendations related to the design of the SWOE 3-D Thermal Model.

2 GENERAL MODELING APPROACH

The energy exchange mechanisms required for a SWOE simulation can be quite complex. Fortunately, simplified assumptions can often be made. Examples of simplifications that can be made are:

- The assumption of steady state conditions
- The assumption of transient energy exchange in which variations are limited to one dimension
- Breaking complex situations into a number of uncoupled models or loosely coupled models

However, not all thermal situations can be simplified and, therefore, the need exists for a three dimensional thermal model (3DTM) in the SWOE program. Since the investment of resources in three dimensional models can be quite large, it is necessary to have a method of assessing when a three dimensional treatment is mandatory and when it is not.

One way to accomplish this is to use existing analytical, multidimensional models developed for applications similar to those in the BTI/SWOE program. They would be used to perform a series of numerical experiments to scope out the problem and define regions where three dimensional effects are important. The models would contain physical processes similar to those required for the 3DTM. The thrust of this effort, then, is to use these models as *design tools* for developing the SWOE 3DTM.

There is another major reason why the modeling approach described here should be followed – to aid in the development of the BTI/SWOE databases. Identifying which physical processes must be handled in a three dimensional fashion will also identify which parameters must be measured on a three dimensional basis and to what degree of accuracy/precision. The number of parameters that have an impact on thermal conditions is substantial and measuring some of the parameters

is very labor intensive. Clearly, the results from these numerical experiments will be important to the modeling and measurement groups within the BTI/SWOE community, as well as the rest of the DoD modeling community.

2.1 Required Capabilities for a SWOE Test Bed Code

The model that should be used as the BTI/SWOE test bed should contain as many of the features that would be encountered in a BTI/SWOE scenario as possible. Some of the more common processes are radiant energy absorption at surfaces, reradiation to the environment, reflected energy from other surfaces, convective transfer to the atmosphere, change of phase within the material, heat conduction, sublimation or gasification, transpiration, densification (compaction), freezing, mass transport by diffusion, percolation, and gas transport. The code should also have the ability to run in either a 1-D or multi-dimensional mode.

SPARTA has a set of thermal response models that have been used to study a variety of processes in laser-material interactions and thermal response studies. These codes are well suited for use as a test bed code. TRAC-3, the most advanced of these codes, has been used in this study and is described in the Appendix.

2.2 Recommended Numerical Experiments

Three situations have been identified as typical of cases where three dimensional effects may be important and we'll be studied under this effort. They are not intended to represent the complete set of situations requiring the use of a multi-dimensional model, but they do represent the set of most commonly occurring situations in which a multi-dimensional approach is thought to be required. They are:

1. Boundaries between different classes of backgrounds
2. Objects embedded in the scene
3. Inhomogeneous distribution of the materials.

The results to be presented in this report are based primarily on environmental conditions for Hunfeld, Germany, on 10 September 1982. Hunfeld is at 50° N latitude and 9° E longitude. This is the day that was selected by the SWOE program for a demonstration of SWOE capabilities in the first year of the effort. Figure 2 displays the air temperatures at shelter height for the day and Figure 3 gives the total solar fluxes. The solar fluxes were calculated using the solar parameterization in the SWOE Preliminary Atmospheric Radiation Package.²

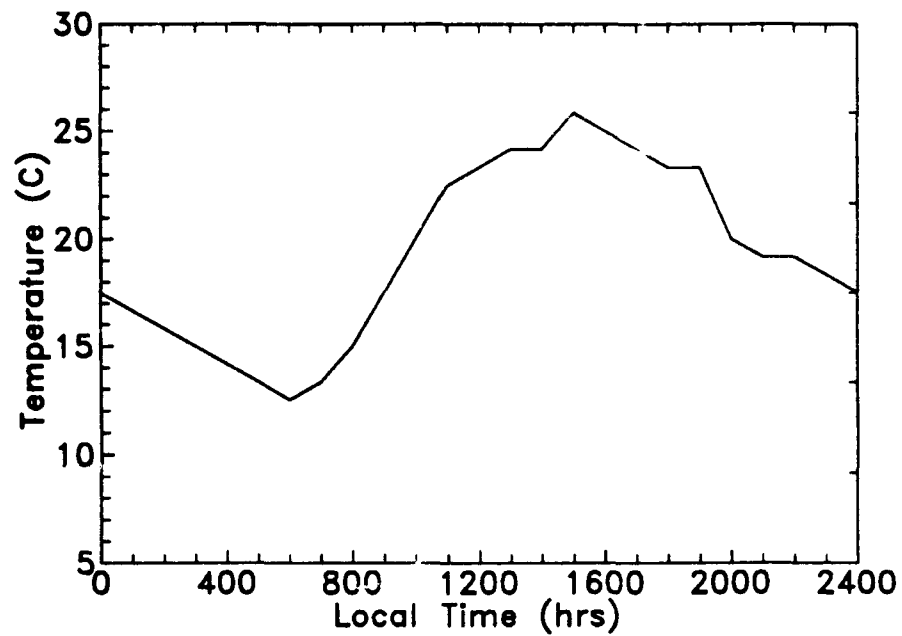


Figure 2. Air Temperature as a Function of Time of Day at Hunfeld, Germany on 10 September 1982

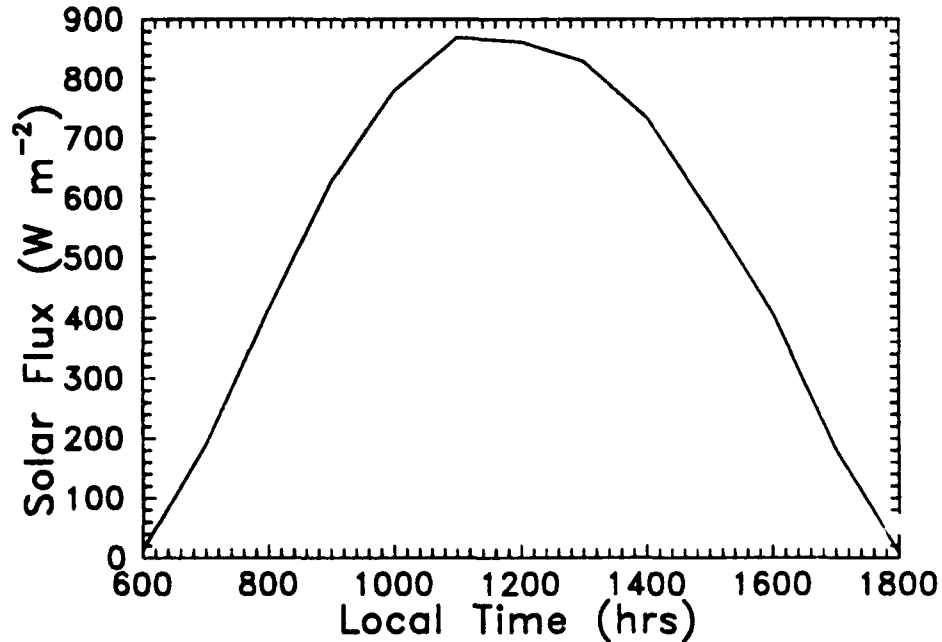


Figure 3. Calculated Total Solar Flux as a Function of Time of Day at Hunfeld, Germany on 10 September 1982

3 BOUNDARIES BETWEEN DIFFERENT MATERIALS

An example of this case is the boundary between different plots of land or a road and shoulder, as shown in Figure 4. Not only can the thermal properties be different on either side of the boundary but so can the mass transfer conditions.

In a 1-D formalism, this situation may result in a discontinuity in the temperature field at the boundary rather than a more gradual transition from one material to the other. This case can be easily modeled with SPARTA's TRAC-3 code. A boundary between different materials can be imposed and the code run for both a 1-D, 2-D, and 3-D situation. The results would aid in demonstrating for which material background classes the effect of the boundary is important and how far away the effect of the boundary is felt.

In this section, a progression is made from 1-D to 2-D to 3-D situations. A comparison is made between the various calculations showing the differences which occur as a result of including the boundary effects.

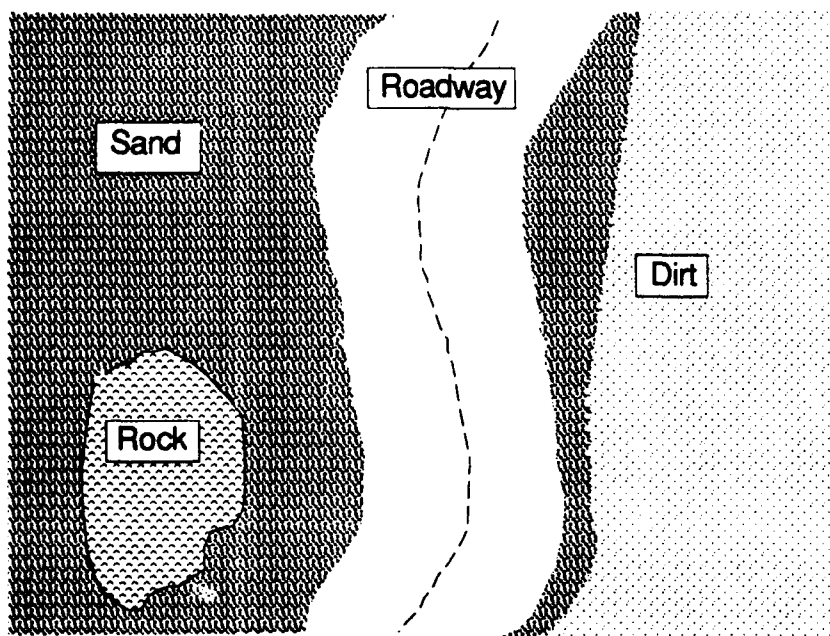


Figure 4. Scene With Marked Boundaries Between Different Material Types

For this investigation, four types of soils and one rock material (granite) were studied. The soils were a sand, and three organic soils with different water and mineral contents. The thermal properties of these soils and rock are given in Table 1. These values were obtained from many sources, but primarily from

TSTM⁴ and Marshall and Holmes.⁵ The solar absorptivity is mainly the shortwave component, whereas the emissivity is primarily the longwave infrared component.

Table 1. Thermal Properties of Soils and Rock Materials

Material Type	Conductivity (W/m-K)	Density (kg/m ³)	Heat Capacity (J/kg-K)	Diffusivity (m ² /s)	Absorptivity	Emissivity	Water Content (%)
Soil III	1.06	1500	1600	4.4×10^{-7}	0.65	0.85	30
Soil II	0.80	1300	1760	3.5×10^{-7}	0.65	0.85	30
Soil I	0.25	1100	1800	2.5×10^{-7}	0.65	0.85	10
Sand	1.20	1200	710	1.4×10^{-6}	0.60	0.85	—
Granite	3.27	2700	800	1.5×10^{-6}	0.70	0.90	—

3.1 One-Dimensional Thermal Calculations

The 1-D calculations were made with a grid consisting of 35 vertical nodes that began at the surface and extended downward into the surface to a depth of 76 cm, as shown in Figure 5. The boundary of the calculation (the bottom nodal element) was used as a heat sink and was kept at a constant temperature of 15 C. The interface between the material and overlying atmosphere (top nodal element, element # 1 in the Figure,) was allowed to react to the ambient air, receive solar and infrared radiation, reradiate to the atmosphere, and undergo convective cooling. Variable spacing was used with the smallest elements placed near the boundaries and interfaces. This was done in order to maintain a near constant temperature gradient across a node. In the case of the atmospheric interface, the temperature difference along the interface can be quite large, therefore, the nodal spacing was made smaller than that found in the interior portions of the material. Conversely, at elements away from interface where the temperature differences are generally smaller, the nodal spacing was made larger. This variable nodal element approach also helps to save computational time because these calculations can be very computationally intensive, especially when the number of dimensions or feature complexity is increased.

⁴ Balick, L.K., Link, L.E., Scoggins, R.K., and Soloman, J.L. (1981) "Thermal Modeling of Terrain Surface Elements," U.S. Army Engineer Waterways Experiment Station, EL-81-2, March, ADA 098019.

⁵ Marshall, T.J. and Holmes, J.W., (1988) *Soil Physics*, Second edition, Cambridge University Press, Cambridge.

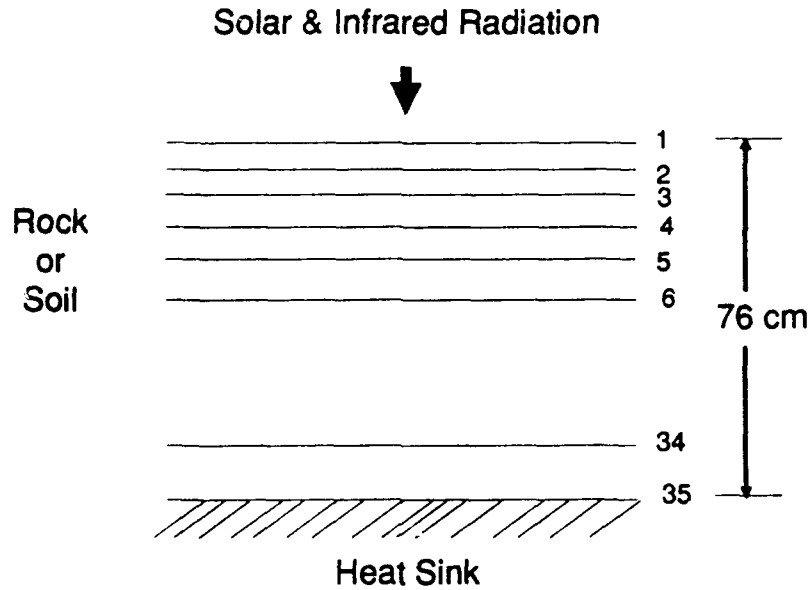


Figure 5. Schematic Representation of the Variable Grid Scheme Used for the 1-D Thermal Calculations

3.1.1 Convective Cooling

For convective cooling, the average heat transfer coefficient, \bar{h} , is the quantity used in the calculation of the convective cooling. Assumptions must be made in order to obtain a value for the heat transfer coefficient. The average heat transfer coefficient is determined as a function of a characteristic length for the object being cooled, L ; the Reynolds number, Re ; and the Prandtl number, Pr . For most regions and times of day, the flow is laminar and the average heat transfer coefficient can be defined as,⁶

$$\bar{h} = 0.664 \frac{k_a}{L} Pr^{1/3} Re^{1/2} \quad (1)$$

where k_a is the conductivity of air (≈ 0.025 W/m-K). The Prandtl number, which gives the ratio of convective to conduction effects, is approximately 0.7 for air at ambient temperatures. The Reynolds number is given as

$$Re = \frac{LV}{\nu_a} \quad (2)$$

where V is the wind speed and ν_a is the viscosity of air. For a 2 m/s wind, the Reynolds number is 1.25×10^5 for a 1 m characteristic length and air at ambient temperatures ($\nu_a = 1.6 \times 10^{-5}$ m²/s). With the Reynolds number given by Eq. (2), the convective cooling coefficient can be given by

⁶ Lienhard, J.H. (1981) *A Heat Transfer Textbook*, Prentice-Hall Inc., New Jersey.

$$\bar{h} = 0.664 \frac{k_a}{L} Pr^{1/3} \left[\frac{LV}{\nu_a} \right]^{1/2}. \quad (3)$$

With these values and Eqn (1), \bar{h} is approximately 5.2 W/m²-K. It is assumed that the wind is from one constant direction and does not change value during the course of the calculations. The convective heat transfer coefficient is assumed to be the same on all surfaces and material types during the day. As a point of interest, the heat transfer coefficient for natural convection on a 30 cm vertical wall is 4.3 W/m²-K.

In the discussion to follow, wind direction is not considered. However, the heat transfer is a function of wind direction because the characteristic length used in the calculation is in terms of the length along the direction of the wind. Therefore, the convective cooling will be different for a wind blowing along the long axis of an object relative to that blowing along a narrower axis.

3.1.2 Discussion of Results

The results of the 1-D calculations are presented as a temperature-time history over a 24 hour period for the various soil and rock types given in Table 1. In all of the cases presented in this study, the calculations were performed for a 48 hour period. The results discussed are for the second day in the cycle, thereby explaining why the nighttime temperatures for the materials are warmer than the ambient air temperatures.

Figure 6 presents the results with and without convective cooling for the sand and granite cases and Figure 7 gives the corresponding results for the three soil cases. Unless specifically stated, all the convective cooling calculations were made with a 2 m/s uniform wind throughout the entire day. The three soil types differ primarily in terms of the amount of moisture in the soil and the results shown in Figure 7 demonstrate the importance of soil water on determining the thermal balance, especially during the daylight hours. Generally speaking, the lower the water content, the higher the daytime temperature.

As shown in Eqn (3), the wind speed affects the amount of cooling with a \sqrt{V} dependence. The impact of wind speed on the skin temperature for three materials as a function of speed is shown in Figure 8. This is an important factor which can lead to a 15° temperature difference.

Table 2 compares the peak temperatures at 1500 hours for all the materials with and without convective cooling effects considered. There are substantial differences in many cases and care should be exercised when defining and designing the thermal model inputs and terrain features.

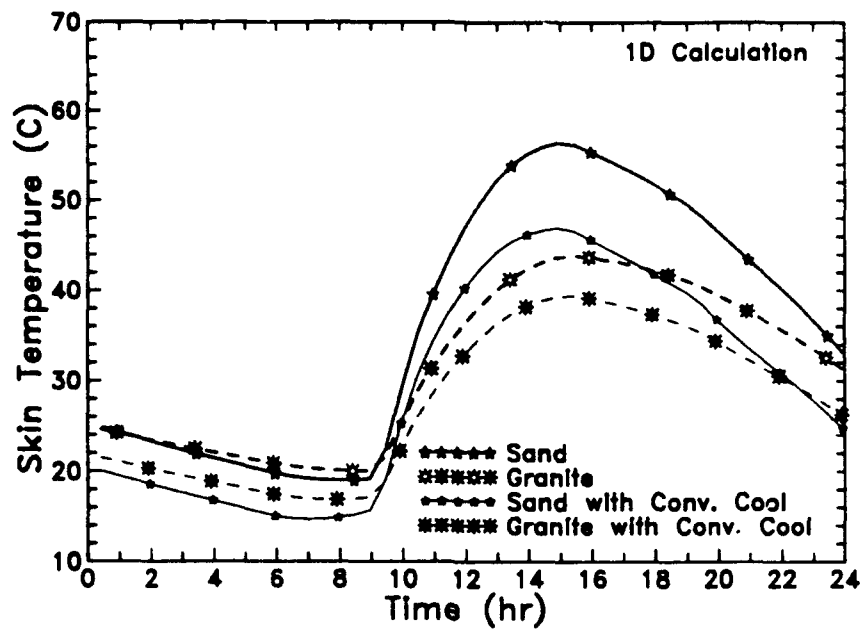


Figure 6. Calculated 1-D Sand and Granite Skin Temperatures as a Function of Time With and Without Convective Cooling Considered

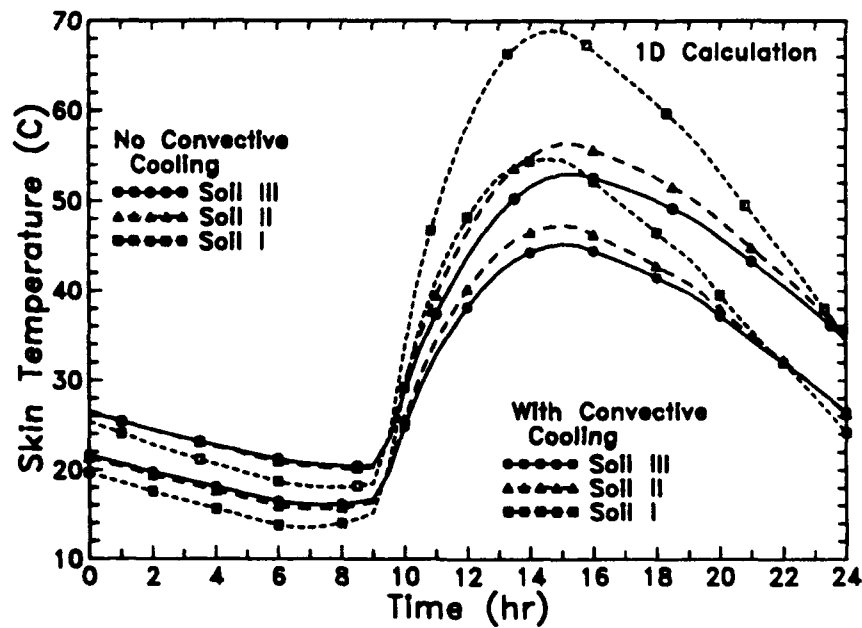


Figure 7. Calculated 1-D Soil Skin Temperatures as a Function of Time With and Without Convective Cooling Considered

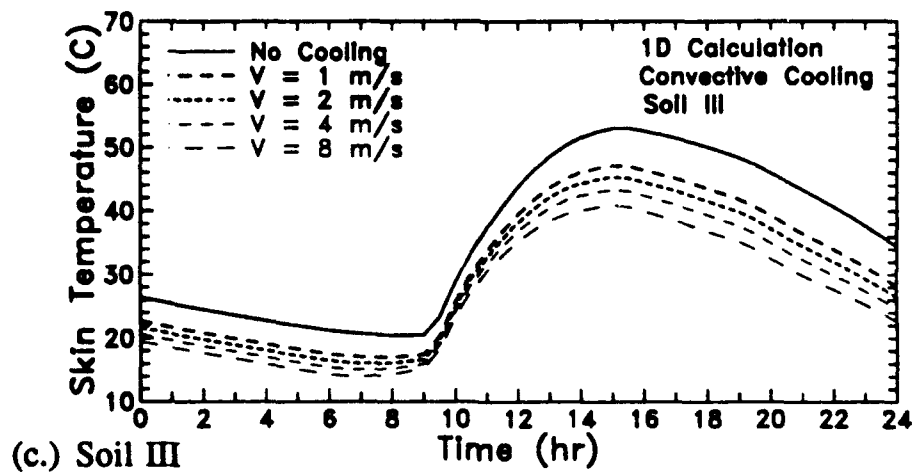
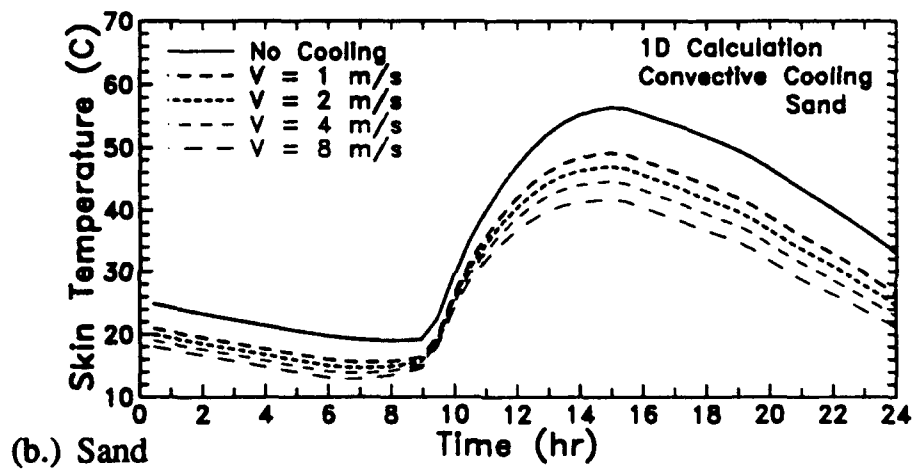
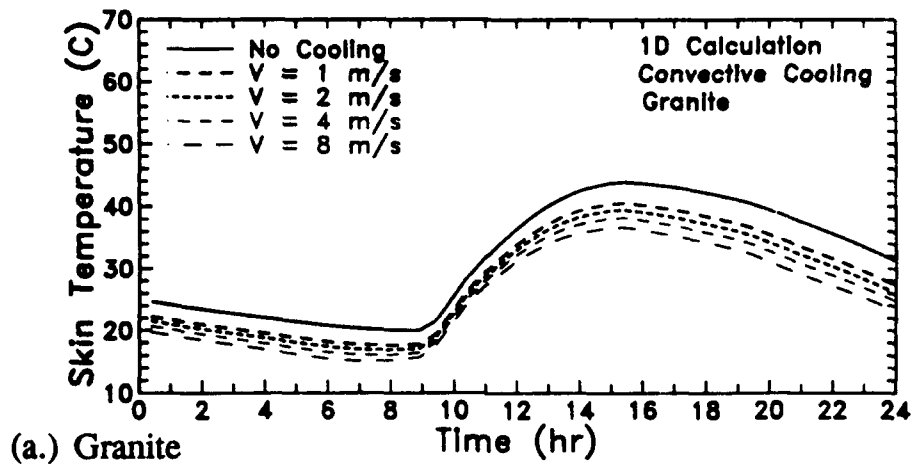


Figure 8. Calculated Skin Temperatures as a Function of Time for (a.) Granite, (b.) Sand, and (c.) Soil Type III Demonstrating the Importance of Convective Cooling

Table 2. Calculated Peak Temperatures With and Without Convective Cooling Effects and the Difference Between the Two Temperatures

MATERIAL	Peak Temperature (No Convective Cooling) (C)	Peak Temperature (With Convective Cooling) (C)	ΔT (C)
Granite	43.5	39.1	4.4
Sand	56.2	46.8	9.4
Soil III	52.8	45.1	7.7
Soil II	56.2	47.2	9.0
Soil I	68.7	54.4	14.3

3.2 Two-Dimensional Thermal Boundary Model Calculations

As was done for the 1-D thermal calculations, the impact of 2-D thermal effects was studied using different materials and soils. For these calculations, a rock was assumed to be buried in the soil, with its top face flush with the surrounding soil surface. Again, variable spacing was used with the smallest elements placed near the bottom boundary and interfaces between the soil and overlying atmosphere, as shown in Figure 9. A buried rock is an easy computational grid scheme to set up within SPARTA's TRAC-3 model since the code is able to automatically generate the finite elements and easily define all the neighboring nodes of each element.

The buried rock 2-D thermal calculations were made with a total of 360 nodal elements. In the vertical, 15 nodes extended down to a depth of 76 cm with variable grid spacing and in the horizontal, 24 nodes were used, also with variable spacing. The bottom nodal elements were used as heat sinks and maintained at a constant temperature of 15 C. All of the top nodal elements were allowed to react to the environment. Calculations were also made with and without convective cooling considered.

3.2.1 Discussion of Results

A rock with a width of 138 cm was assumed for our default conditions. Calculations were made with the rock embedded in sand and in soil type III. Calculations were performed for an interface between the soil material and the rock and a mirror image of the results to simulate the interface on the other side of the rock.

Figure 10 (a.) shows the calculated 2-D skin temperatures as a function of time for the case with the rock embedded in the sand and Figure 10 (b.) shows the results for the rock embedded in the soil type III. Convective cooling was assumed in all cases. In each Figure, results are given for the temperatures at locations well within the rock and the soil material and near the respective interfaces. The

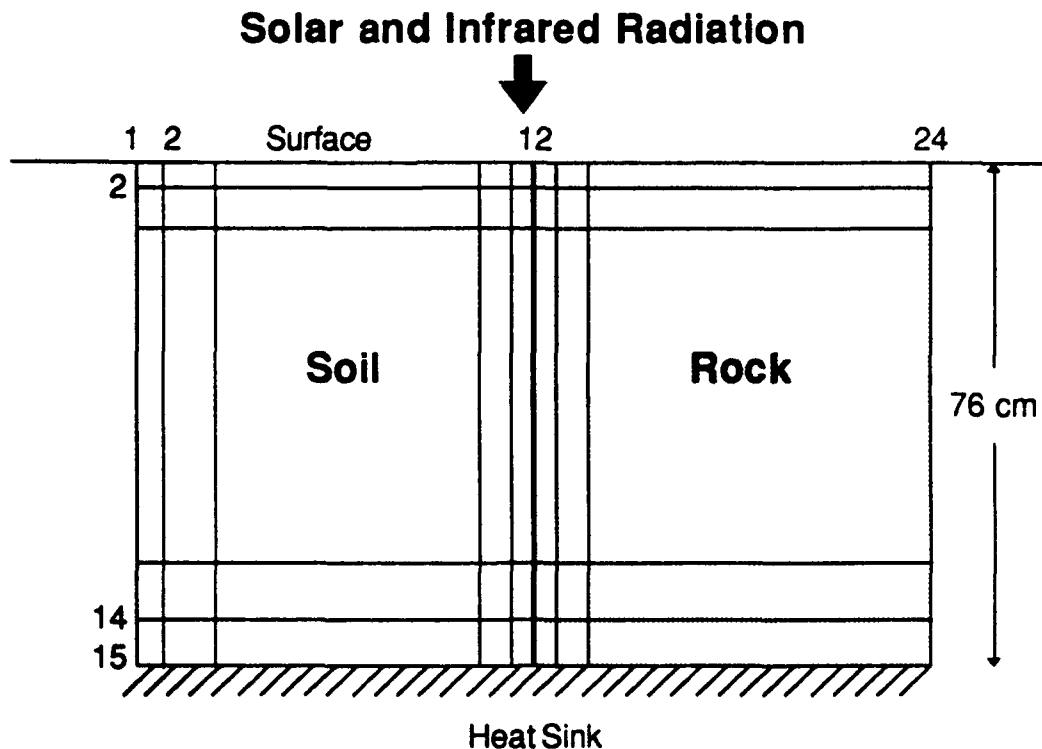


Figure 9. Grid Scheme Used for 2-D Calculations of a Buried Rock

intent of displaying these results is to show the role of the lateral heat conduction. For comparison purposes, the 1-D calculations for the rock and soil materials are also shown. (Note that the slight differences between the sand/granite and granite/sand temperatures is due to the temperatures of each being calculated at the nodal midpoint.)

The results in the Figures demonstrate that for locations in the rock away from the influence of the thermal gradients caused by lateral heat conduction at the interfaces, there is little difference between the 1-D and 2-D calculations. This indicates that for points well embedded in a material and away from the influence of lateral heat conduction from an adjacent material, that 1-D calculations are sufficient. This suggests that for large extended objects, such as roadways, 1-D calculations would be sufficient at locations well away from the interface. However, near the interface, the effects of horizontal conduction are important. This is evident in Figure 11 which displays the temperatures along a line that passes through the interfaces.

The results in Figure 11 are for 1500 hours and show the results for the rock in

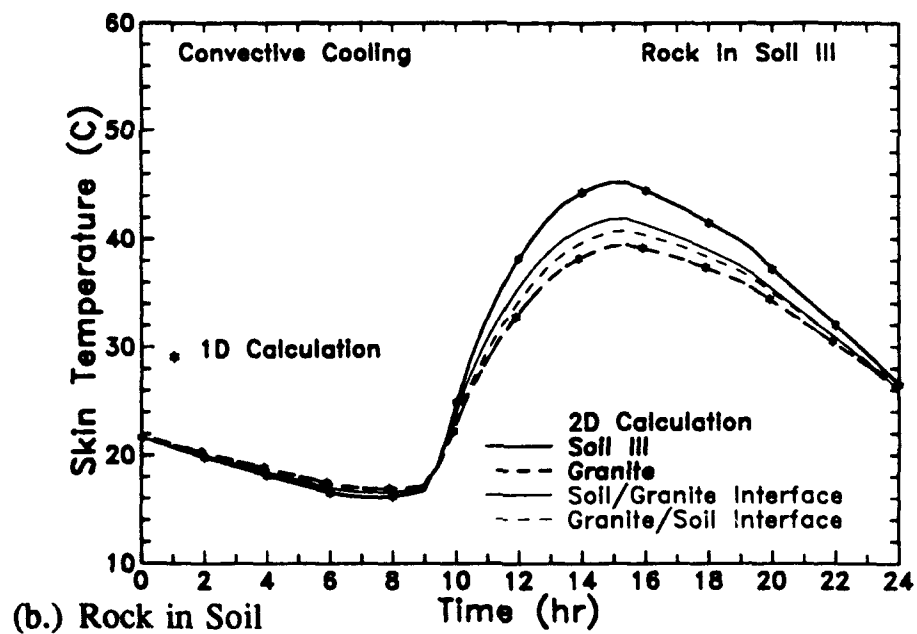
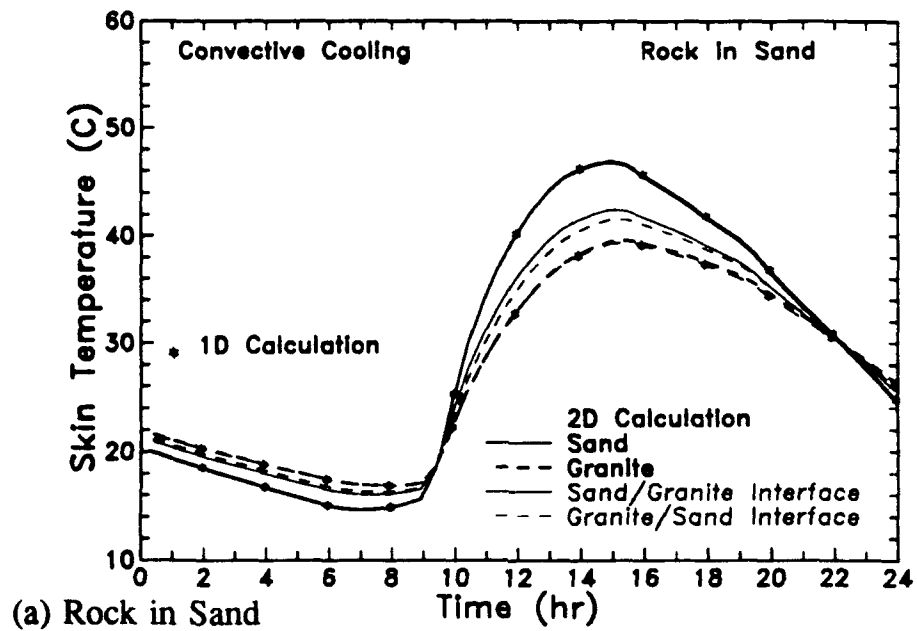


Figure 10. 2-D Skin Temperatures as a Function of Time for a Rock Embedded in (a.) Sand and (b.) Soil Type III. The asterisks are the results for the 1-D calculations

sand and rock in soil III cases. The dashed lines at the interface represent the step function appearance one would get if 1-D calculations were used. A temperature discontinuity of several degrees would result at the interface rather than the gradual transition as shown from the 2-D calculations. The transition occurs, for these simulations, over several tens of centimeters. As shown in Figure 12, however, the magnitude of the temperature change and the distance over which the transition occurs varies as a function of time of day and, most likely, season.

In the preceding discussion, generic terms like "well embedded in" and "near" have been used to describe distances. Determining the distance over which horizontal heat conduction is important is difficult because it would be dependent upon the materials involved and the environmental conditions driving the thermal energy exchange. However, to obtain a very rough estimate of the "zone of influence" of 2-D and 3-D effects, the heat conduction relation for an infinite composite solid can be utilized.⁷ The solution assumes initial temperatures within each material which is followed in time. Our problem is much more complex, but this gives a rough order of magnitude solution which is dependent only upon the time interval, t , and the thermal diffusivity, κ , of the particular materials. The distance from the interface where the temperature of a material reaches 90% of its 1-D value is given by

$$x_{90\%} = 1.16(2\sqrt{\kappa t}). \quad (4)$$

In the results reported here, the time interval is one hour.

For the granite and sand, the respective zones of influence calculated from the above relationship are approximately 17 cm. The zones of influence shown in Figures 11 and 12, based on the full numerical solution, are on the order of four times larger and suggest that a "rule of thumb" of about four times $x_{90\%}$ could be used to establish a zone of influence where multi-dimensional calculations are required. However, additional studies with other materials and environmental conditions should be performed before this rule of thumb is accepted.

3.2.2 Sensitivity of Thermal Field to Buried Rock Width

The width of an object can have a significant impact on the thermal response near an interface. There is a minimum width for a buried rock to have a region where the temperatures can be described by a 1-D calculation. This can be seen in Figure 13 where temperature results from 1500 hours, the time of peak temperatures for this set of environmental conditions, are shown with a rock of different widths from 138 cm down to 12 cm. In the Figure, the temperatures are taken along a

⁷ Carslaw, H. S. and Jaeger, J. C. (1959) *Conduction of Heat in Solids*, Second Edition, Oxford University Press, Glasgow.

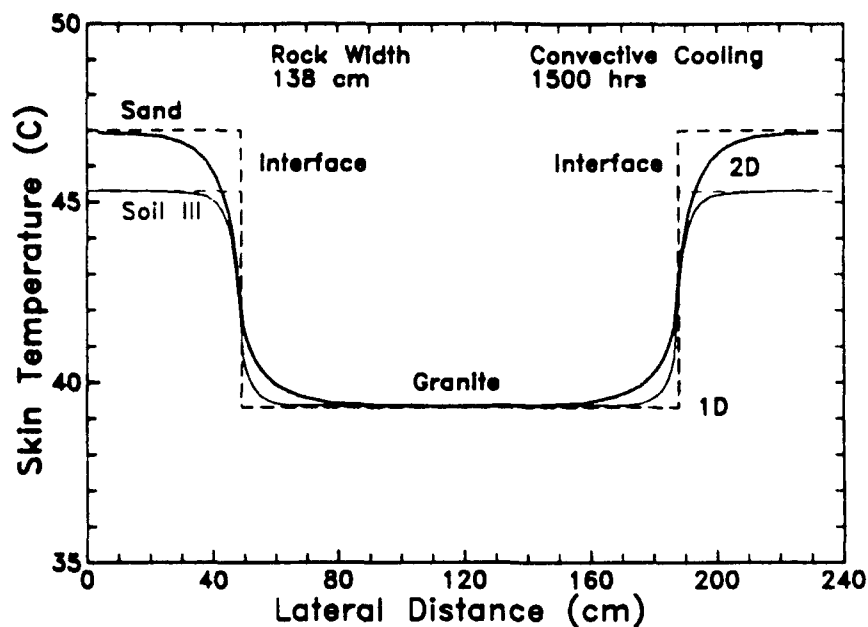


Figure 11. Temperatures at 1500 Hours Along a Line Passing Through a Granite Rock Embedded in Soil

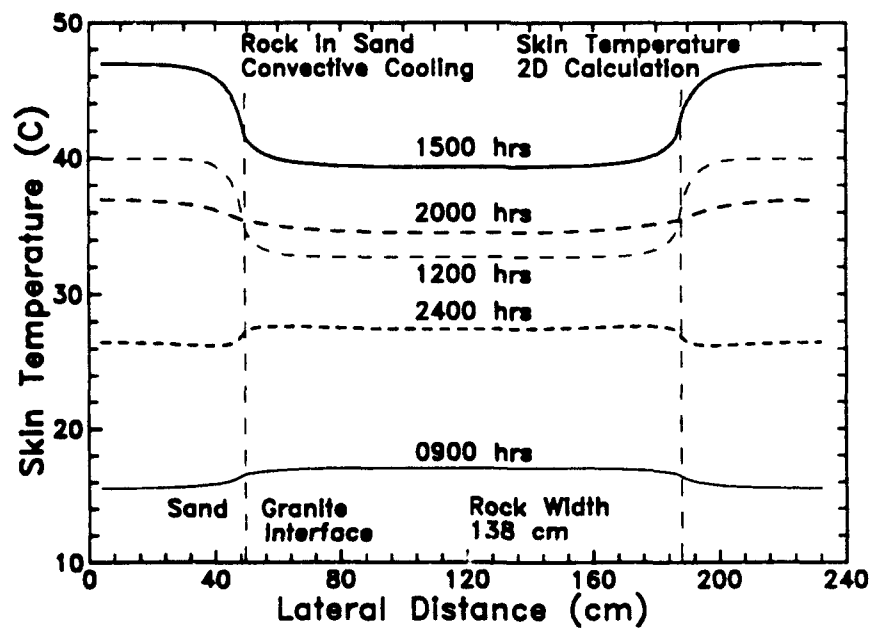


Figure 12. Temperatures Along a Line Passing Through an Embedded Rock as a Function of Time of Day

line passing through the sand and embedded rock. The results shown included radiative cooling, but did not include convective cooling.

As the width of the rock decreases, the thermal conditions in the sand have more and more of an impact on the peak temperatures within the interior portions of the rock. In the results shown, a rock must have a width of about 66 cm or greater to exhibit temperatures on the order of those found by 1-D calculations. This minimum width is on the order of four times $x_{90\%}$.

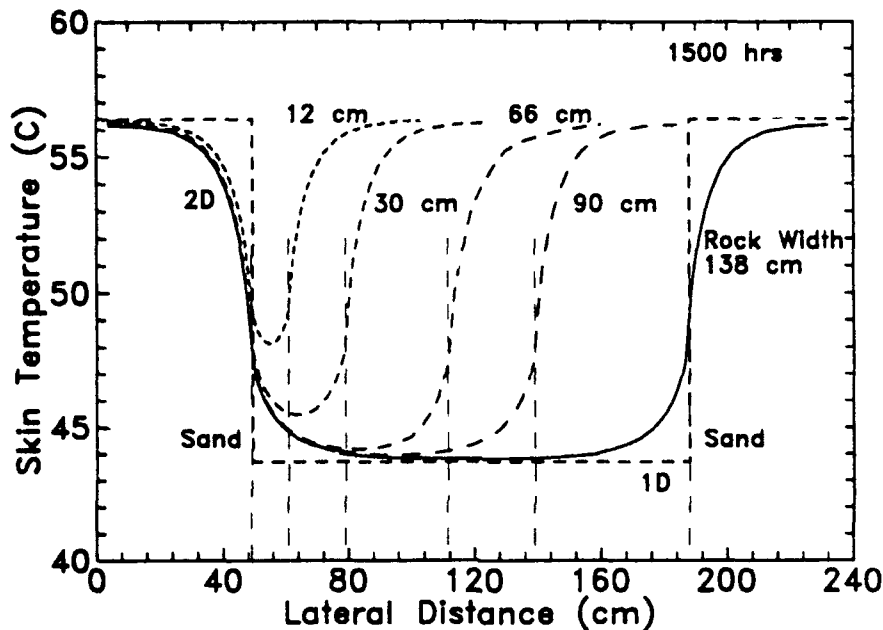


Figure 13. Impact of Rock Width on 2-D Temperature Calculations

4 THREE DIMENSIONAL OBJECTS EMBEDDED IN THE SCENE

An example of a complex scene with embedded three dimensional objects is given in Figure 14 in which a rock is embedded in soil and a roadway with underlying ballast are present. Other more complicated examples could include the presence of buildings, vehicles, and vegetation. When vehicles are present, the effect can be complicated further if the vehicle is operating, thereby making it another infrared energy source in the scene.

In order to study the role of 3-D objects embedded in a scene, two situations were considered. The first is a finite rock embedded in soil and the second, one in which the rock is placed on top of soil. In both cases, a sandy soil was assumed. These cases are much harder to set up than the previous ones because the interfaces between the rock and the soil must be carefully "put together" and specified. In

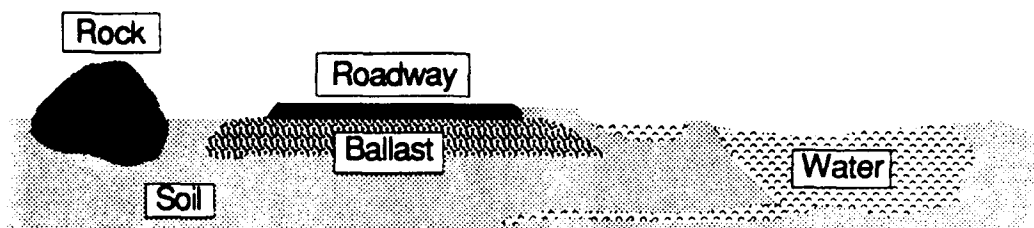


Figure 14. Complex Scene With Embedded 3-D Objects

order to simplify the calculations, a 3-D rock was constructed and modeled with axial symmetry assumed.

4.1 3-D Rock Embedded in Soil

The primary effect of embedded objects is that their "thermal footprints" can be considerably larger than their spatial footprints. During the day when the object is sunlit, it can act as a heat source for the surrounding materials while at night it can act as a heat sink or source. In a 1-D treatment, temperature discontinuities would be produced. In a full 3-D approach one can determine the extent of the thermal footprint of various types of objects. These calculations can be performed for different types of objects and surrounding materials.

For the case of an embedded 3-D scene feature, a rock was assumed to be buried in soil, as noted in Figure 15. The rock that was modeled was 131 cm wide, 64 cm deep, and 348 cm long. (Note that the rock shown in the Figure is only 174 cm long. Mirror symmetry was assumed in order to extend the rock to the full 348 cm length.) The calculations assumed 12 cm of soil under the rock, 29 cm of soil on the right and left (relative to the Figure), and 24 cm of soil on either end. The total number of computational nodal elements was 4800 – 10 nodes in depth, 30 nodes across, and 16 nodes back. Even this large a number of nodes does not allow for a great deal of resolution considering the size of the rock and the soil surrounding it.

Results from the 3-D calculations have been compared from a number of vertical slices through the rock. Figure 16 shows the relative positions of the slices through the rock. Figures 17 and 18 compare the skin temperatures as a function of time at various points on the surface along these slices. In Figure 17 (a.), the temperatures as a function of time on the surface of the rock at positions near the sand/rock interface are shown and in Figure 17 (b.) the temperatures as a function of time for positions from the interior portions of the rock are compared. In Figure 18 (a.) the temperatures along slices A and D from points near the rock/sand interface and interior are compared and in 18 (b.) the same temperatures for slices B and

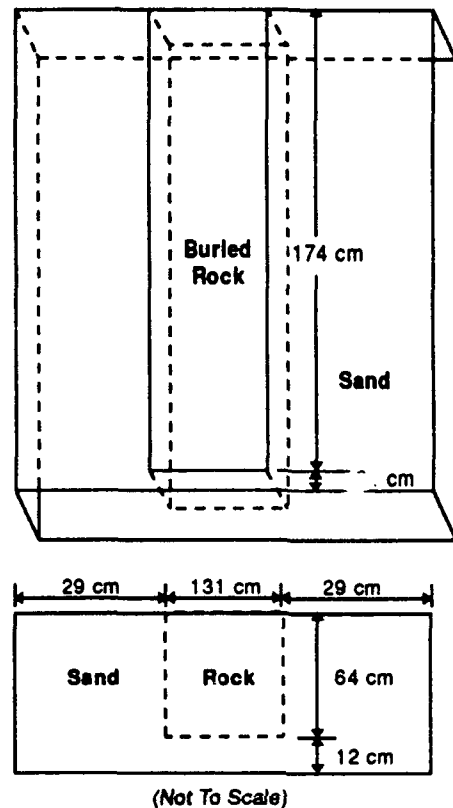


Figure 15. Schematic Representation of the Buried Rock Model Used in the 3-D Calculations of a Rock in Soil

D are compared. In 18 (a.), the temperatures from the points on slice A are indistinguishable because of their proximity to and influence from the surrounding sand.

These results indicate that horizontal conduction across the interface is more important than conduction along the axis of the rock. At a reasonable distance from the edges of the rock, the temperature distribution within the rock is similar to that produced from the 2-D calculations. Unfortunately, there is no easy way to determine what this "reasonable distance" is. To a first approximation, however, one could most likely perform 2-D calculations on each of the sides without a serious loss of thermal detail.

4.2 3-D Rock Placed On Top of Soil

In order to study the role of 3-D objects embedded in a scene, a rock placed on top of the sandy soil has been modeled. This is a much harder case to set up than the previous ones because the interfaces between the rock and the sand must be carefully "put together" and specified. In order to simplify the calculations, a 3-D

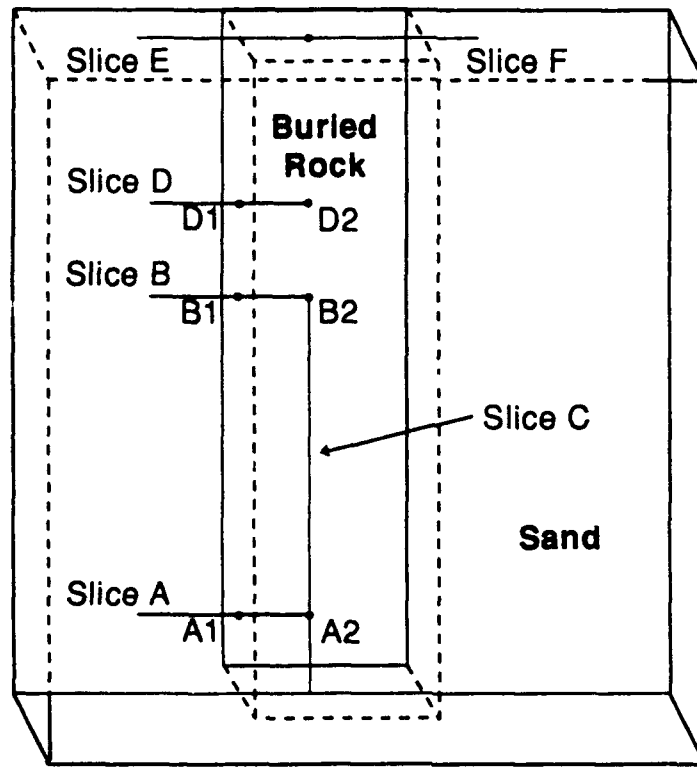


Figure 16. Positions of Slices and Reference Points on the Surface Used in the Buried Rock 3-D Thermal Calculations

rock was constructed and modeled with axial symmetry assumed. In this case, the calculations could be done using the 2-D version of TRAC-3. The modeled scene is illustrated in Figure 19. The calculations consisted of a total of 167 elements, 72 for the rock and 95 for the sand underneath. Again, a variable grid spacing was used with finer resolution at the interfaces and boundaries.

The thermal calculations of the rock on sand are more complex than the rock embedded in sand. The primary reason is that there are more surfaces which can interact with the ambient thermal fluxes and radiation.

The solar irradiance incident on the surfaces was precalculated using the Preliminary SWOE Atmospheric Radiation Package² and provided as input to the code. It was assumed that the various vertical walls were facing due east, west, north, and south. Figure 20 shows the total solar fluxes as a function of time incident on the various vertical faces and the top horizontal surfaces (rock and surrounding sand). Figure 21 displays the skin temperatures as a function of time for the top of the rock, and the east, south, and west faces.

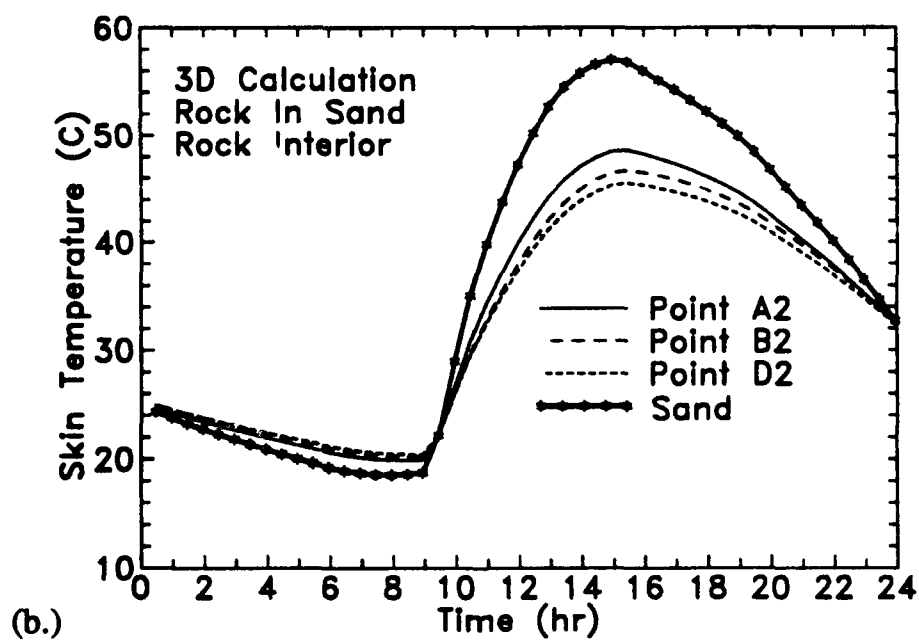
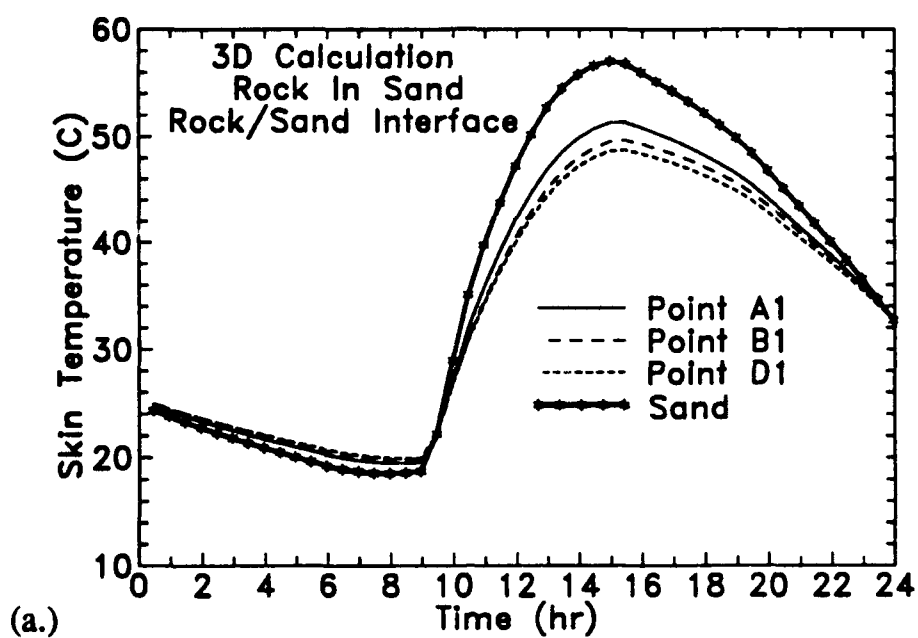
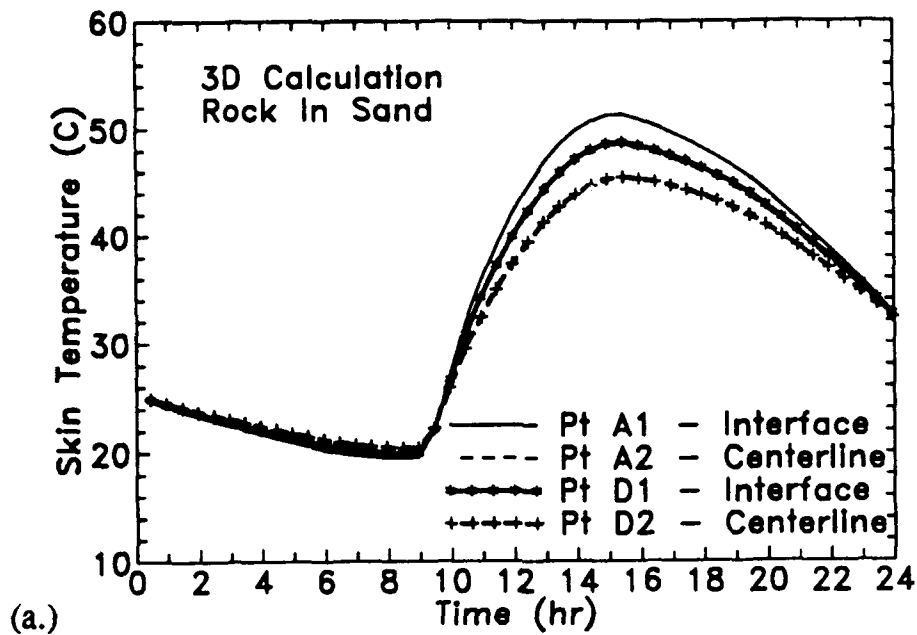
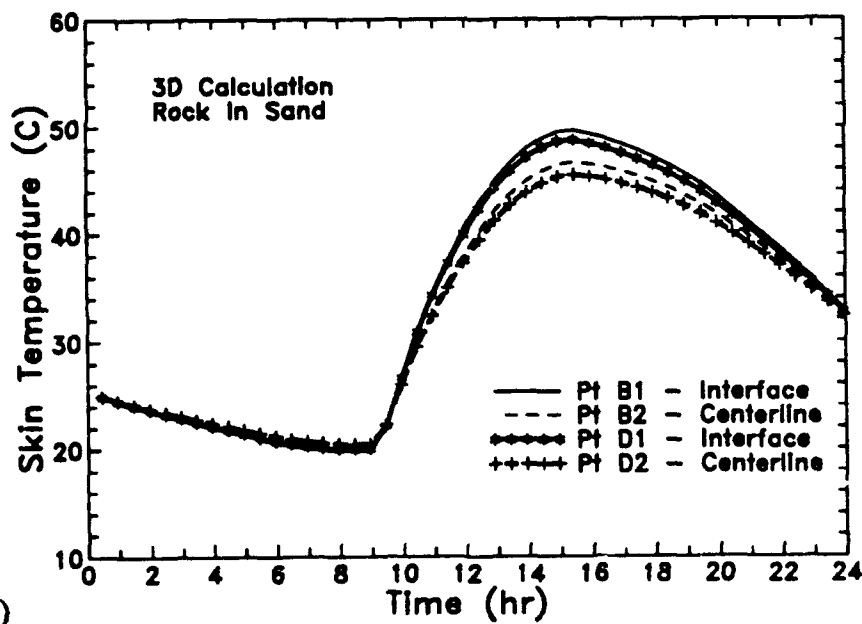


Figure 17 Skin Temperatures as a Function of Time for Different Points on the Surface of a Rock Buried in Sand. (a.) Temperatures at the rock/sand interface and (b.) at the midpoint of the rock surface



(a.)



(b.)

Figure 18. Comparisons of Skin Temperatures as a Function of Time Near the Sand/Rock Interface and the Rock Interior for the 3-D Thermal Calculations of a Rock Buried in Sand. (a.) Temperatures from points along slices A and D and (b.) slices B and D

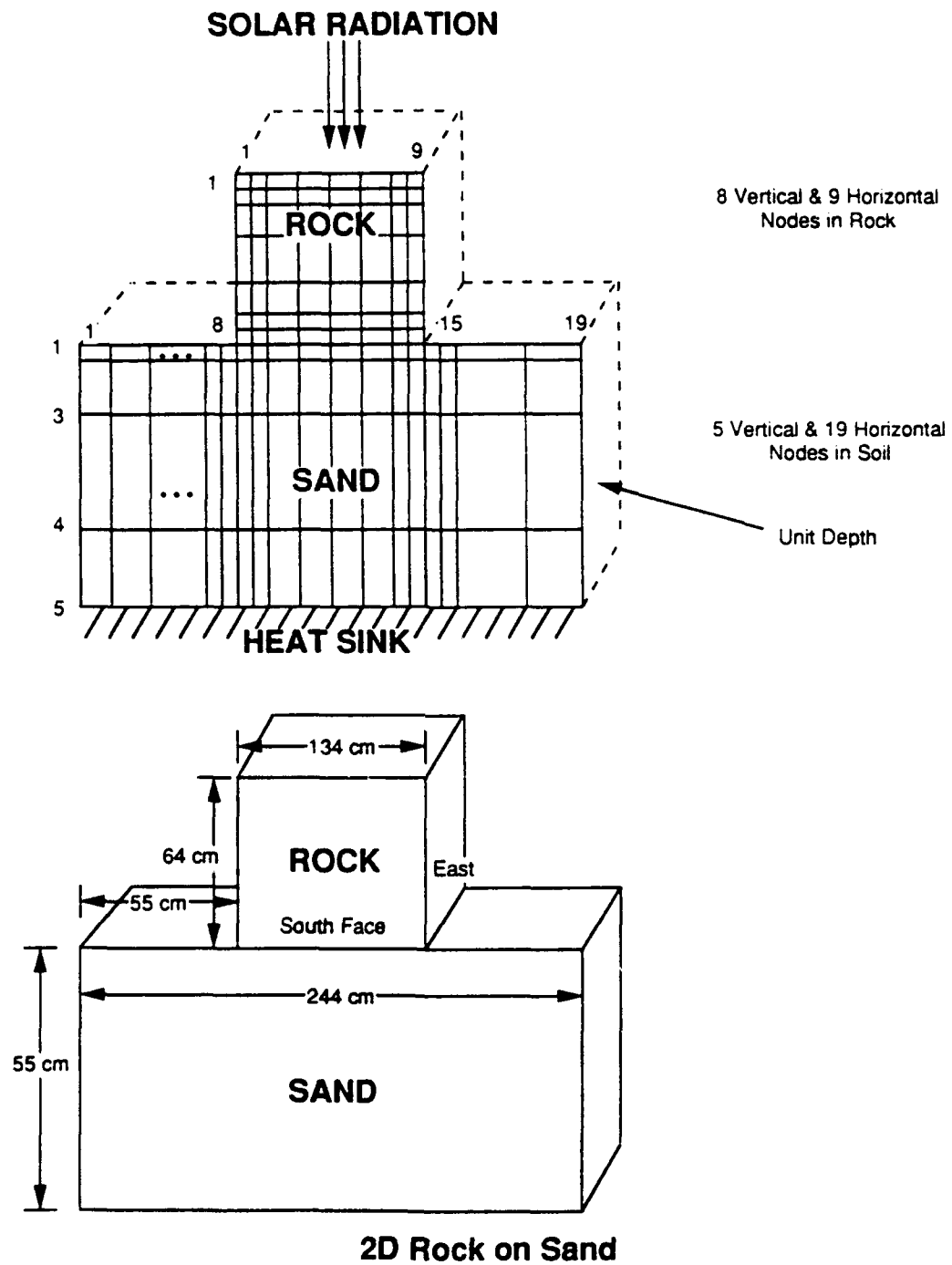


Figure 19. Schematic Representation of a Rock Place on Top of Sand

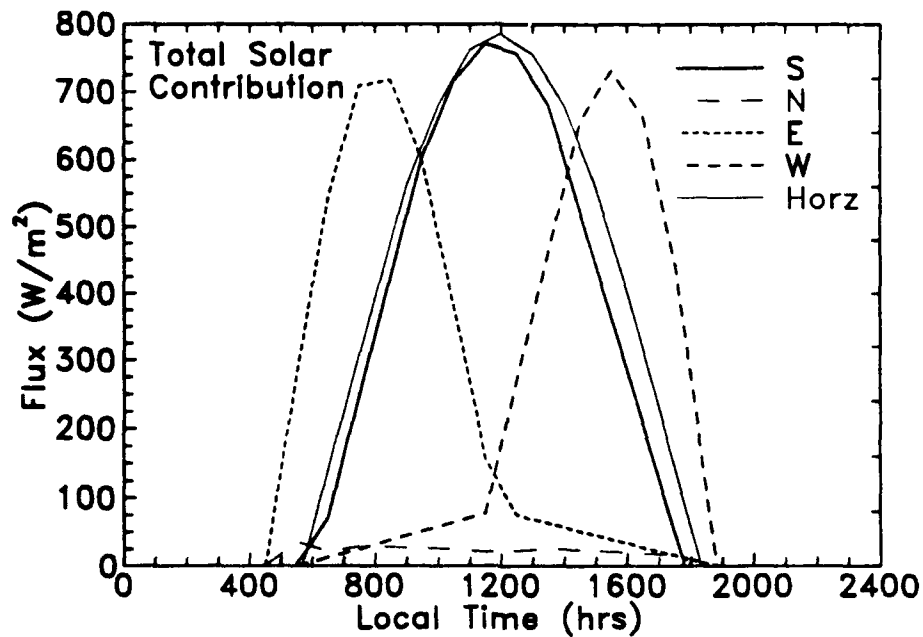


Figure 20. Total Solar Fluxes Incident on the 3-D Rock Faces as a Function of Time of Day

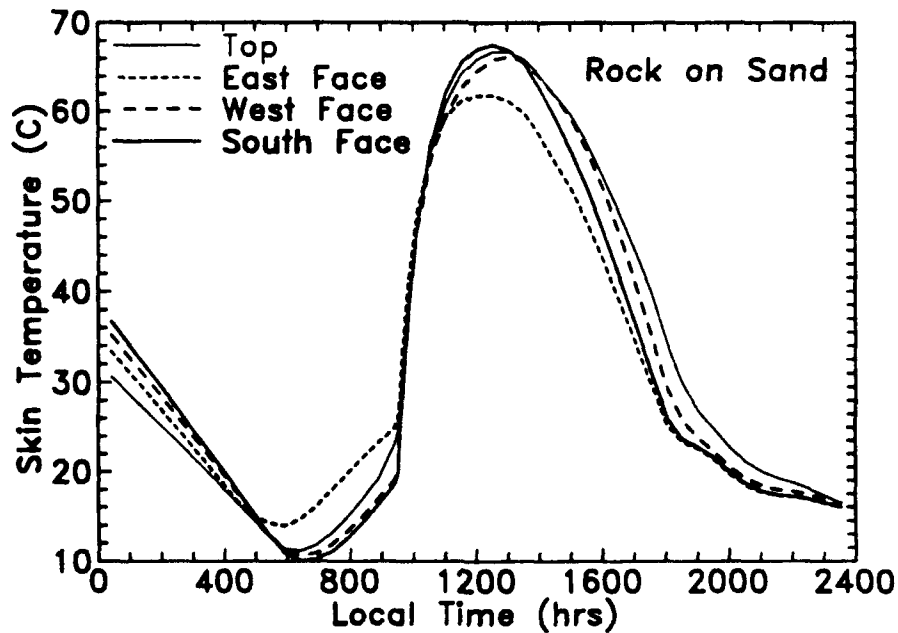


Figure 21. Calculated Skin Temperatures as a Function of Time at Positions at the Midpoint of the Different Rock Faces. The calculations assumed convective cooling and no shading

As shown in Figure 21, the temperature of the various rock faces is dependent on the energy distribution upon the face. The various vertical faces change places in terms of which is the hottest during the day as the solar position changes. This will result in a complicated temperature pattern for the top face.

5 INHOMOGENEOUS DISTRIBUTION OF MATERIALS

This situation is most representative of the "real world" and may also be the most difficult to account for. For example, soil properties will vary greatly from one horizontal location to another within a given field as well as vertically. However, obtaining the data to properly account for these subsurface variations would be an extremely costly venture.

For the purposes of this discussion, inhomogeneous distributions of materials will refer to two situation. The first situation involves variations in the stratification of soils and the second variations in the composition of a designated surface type.

An idealized representation of a soil cross section composed of nonuniform stratification of soils is sketched in Figure 22. The sketch shows several strata of uniform thickness. One of the strata is represented by a periodic variation of the material in the lateral direction. The idealized configuration is not chosen as a faithful representation of realistic scenario, but rather as a model configuration in which the impact of inhomogeneous distributions of materials within a surface on the surface temperature can be studied.

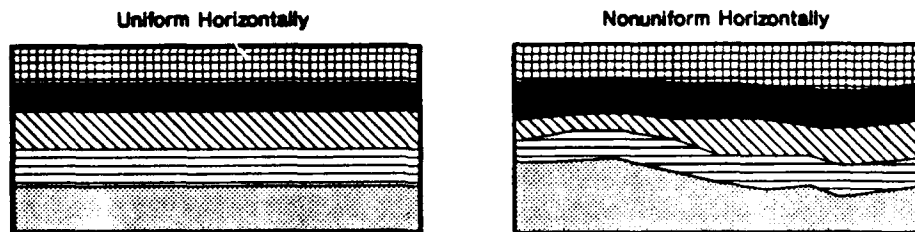


Figure 22. Sketch of a Soil Cross Section With Uniform and Nonuniform Soil Stratification

The second situation being considered addresses the issue of how homogeneous is a "homogeneous" surface. In the SWOE concept, surfaces are divided up into a series of polygons and assigned a surface material code with average material properties. The sizes of these polygons is determined by the assumed resolving power of the sensing systems being studied. The finer the resolving power, the

smaller the polygons and, the more accurate the material properties have to be. Therefore, the definition of how homogeneous a given surface is will depend upon how well the surface can be resolved by the sensing system.

To study the importance of inhomogeneous distributions of materials, calculations were made using the SWOE Interim Thermal Model² and the environmental conditions used previously. In the calculations, the material properties were perturbed the same relative amount (10%) and the results scaled to determine which properties were most important in determining the surface temperature. The scaling was performed by taking the ratio of the temperature difference for a given perturbation to the maximum temperature difference from the set of perturbations. The results are listed in Table 3 and given in terms of daytime and evening conditions.

Table 3. Relative Importance of Surface Temperature to Changes in Material Properties. The values shown are based on a 10% change in the listed material property

MATERIAL PROPERTY	RELATIVE IMPORTANCE (Daytime)	RELATIVE IMPORTANCE (Evening)
Surface Albedo	1.00	-
Emissivity	0.85	1.00
Bulk Density of Dry Materials	0.41	0.48
Density of Dry Materials	0.25	0.29
Heat Capacity of Dry Materials	0.19	0.22
Thermal Conductivity of Dry Materials	0.13	0.16

The Table shows that the surface albedo and emissivity, the two material related terms that control how much energy gets into and out of the surface, are the two most important parameters effecting the surface temperature. The bulk density of dry materials, density of dry materials, heat capacity of dry materials, and thermal conductivity impact the heat conduction within materials and are of significantly lesser importance. What these results demonstrate is, that in terms of calculating the surface temperature the nature and description of the top surface is more important than the character of the subsurface materials.

Additional studies were performed in which the number and thickness of layers was varied and the impact on surface temperature again assessed. In those studies,

when the thickness of the top soil layer exceeded a few centimeters, the surface temperature was essentially not affected by changes in the properties of the underlying layer. These results demonstrate that variations in the material properties of the surface materials has a minimal impact on the surface temperature.

However, in terms of describing the thermal structure within the soil, the characteristics of the subsurface materials are very important. This can be illustrated in Figure 23 which displays soil temperature data taken during the SWOE Thermal Analysis and Modeling Program (*c.f.*⁸)

The data were measured by thermocouples placed 1 and 20 cm below the surface at two locations which were within 10 meters of one another. The thermocouples were placed at location with similar surface characteristics. Figure 23 (a.) shows that the soil temperatures 1 cm below the surface at the two locations are very similar. However, as shown in Figure 23 (b.), the temperatures 20 cm below the surface exhibit significantly different thermal responses, presumably due to differences in the material compositions and distributions at that level.

The point of these results is to demonstrate that if one only wants to understand the surface temperature response, one most likely does not have to model the 3-D variations in the subsurface materials. However, if one wants to understand the temperature distribution and response within the materials as well, a multi-dimensional modeling treatment and data collection effort is called for.

6 SUMMARY AND RECOMMENDATIONS

6.1 Summary

The modeling and understanding of the radiant field from natural backgrounds is a complex undertaking due to the great variability in scene elements. The physical processes producing the scene temperatures, the source of the radiant field, as well as many of the objects in the scene, are three dimensional in nature so a full 3-D treatment of the physics is necessary in order to properly describe the radiant field. However, the theoretical requirement for a 3-D treatment of the physics must be balanced against the practical realities of what 3-D processes are actually important and if proper and complete data resources are available to justify the detailed calculations.

This study focused on understanding when multi-dimensional modeling of temperatures is required. Three situations were studied where multi-dimensional effects

⁸ Hummel, J.R., Paul, N.L., Jones, J.R., Longtin, D.R. (1991) "STAMP - The SWOE Thermal Analysis and Measurement Program: Summary of the 1990 Field Tests," Phillips Laboratory, Hanscom AFB, Massachusetts, PL-TR-91-2242, 8 October.

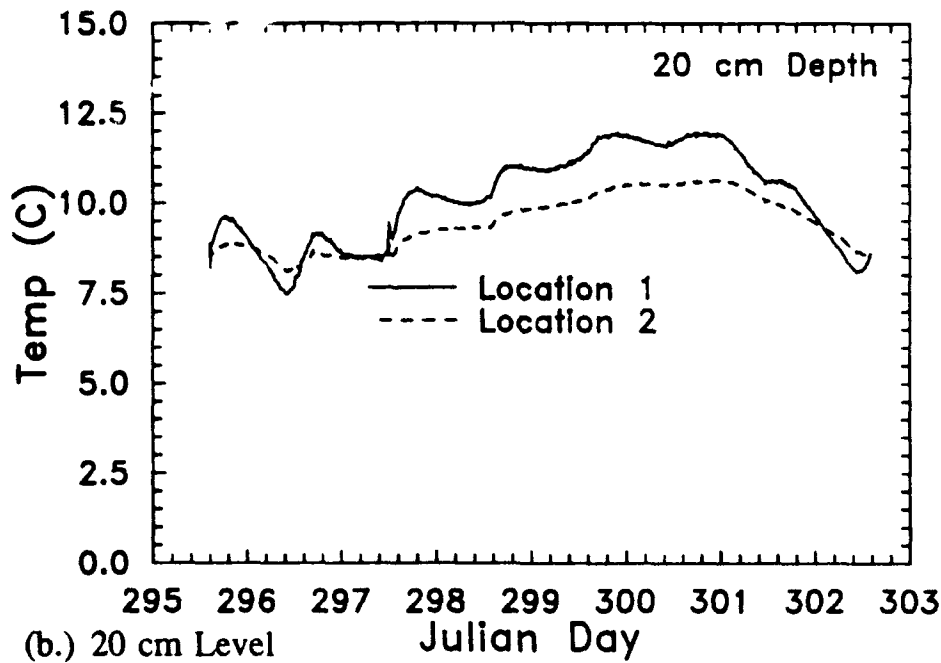
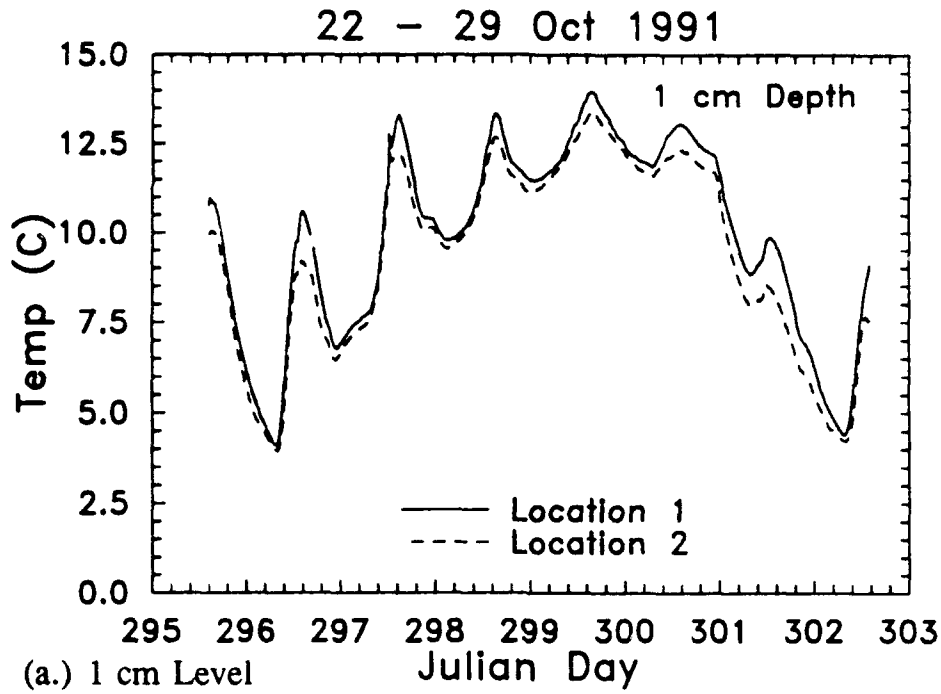


Figure 23. Comparison of Soil Temperatures as a Function of Time as Measured at Two Closely Spaced Locations at (a.) 1 cm and (b.) 20 cm Below the Surface

are important. They are:

1. Boundaries between different classes of materials
2. Objects embedded in the scene
3. Inhomogeneous distribution of materials.

6.1.1 Boundaries Between Different Classes of Materials

When this situation is modeled in a 1-D format, sharp discontinuities result at the interface between the materials. This is unrealistic and would result in incorrect analyses of temperature variations in a scene. As a result of lateral heat conduction, the temperature change is more gradual. Results were presented to demonstrate that the distance over which this transition occurs is a function of the differing materials, time of day, and in the case of a 2-D infinitely long object, the width of the object.

6.1.2 Objects Embedded in Scenes

Studies were made of the impact of objects in an energy balance simulation. Two conditions were studied, a rock embedded flush in a soil and a rock on top of the soil. The case of the rock embedded in soil was simulated using both 2-D and 3-D calculations.

In the case of the buried rock, it was demonstrated that the effects of lateral heat conduction impacted the temperature distributions both within the rock and in the surrounding soil, such that "thermal footprint" of the objects were larger than the spatial footprint and these footprints varied with the time of day. For the rock placed on top of the soil, the temperature distribution on the various rock faces is dependent upon the solar loading on the rock faces. This means that not only must the temperature distributions within the object be calculated in a 3-D manner, but the energy loadings into and out of the object must also be modeled in a 3-D fashion.

Both simulations were complex and time consuming to implement. Constructing the 3-D objects and developing a proper numerical grid system is a non-trivial task. The 3-D models are very computer intensive since there are many nodal points which must be used in the thermal calculations.

In the case of the rock embedded flush in the soil, the thermal response was similar to that of the infinitely long 2-D object mentioned above. The rock placed on the top of the surface was, by far, the most complex situation to model. The solar energy on each of the rock faces had to be taken into account in order to properly handle the energy distribution within the rock. As a result, the temperature of the faces was highly dependent on which face was in the sunlight.

6.1.3 Inhomogeneous Distribution of Materials

This situation is most representative of the "real world" and also the most difficult to account for in a modeling context. Soil properties will vary greatly from one horizontal location to another within a given field as well as vertically. Obtaining the data to properly account for these subsurface variations is an extremely costly venture.

A set of sensitivity calculations was performed to determine which material properties are most sensitive in controlling surface temperature. The surface albedo and emissivity were found to have the greatest impact on surface temperature. The other material properties were significantly less sensitive.

6.2 Recommendations

The design of a multi-dimensional energy balance model is not for the faint of heart. The results of this study indicate that it is not necessary to perform multi-dimensional calculations at all locations within a scene. Instead, the model should consist of a system in which 1-D calculations are performed for uniform surfaces and materials and the multi-dimensional calculations reserved for only those situations that physically warrant them and for which the data requirements for them can be met. The situations that most fit these conditions are boundaries between materials and 3-D objects placed in a scene. The boundaries can be handled in a 2-D context while the 3-D objects must be handled with a full 3-D model.

6.2.1 Boundaries Between Materials

Away from boundaries, the 1-D calculation is more than sufficient for the calculation of the thermal signature. It is only near the object or boundary where 2-D analyses are necessary. It is here where thermal gradients can affect the radiance field as seen by particular sensors. Additional research is required to help establish at what distance from a boundary one must switch from a 1-D to a 2-D calculation.

6.2.2 Presence of 3-D Scene Objects

The hardest part of modeling 3-D objects is the establishing of the geometric model and corresponding numerical grid. To facilitate this process, it is recommended that generic objects with pre-established geometries and grid schemes be used. One could then do a single or limited set of thermal calculations of these generic objects and then replicate them in a scene simulation.

6.2.3 Inhomogeneous Distribution of Materials

While the inhomogeneous distribution of materials is a very common occurrence, having the data resources to justify a multi-dimensional calculation are rarely satisfied. Therefore, it is recommended that when the desired output product is the surface temperature, this situation be handled by applying statistical "texture" functions to the results of 1-D calculations. However, if one also wants to calculate the thermal response and temperature distribution within the material, a multi-dimensional model and data collection effort may then be necessary.

References

1. Balick, L.K., Hummel, J.R., Smith, J.A., and Kimes, D.S. (1990) "One Dimensional Temperature Modeling Techniques for the BTI/SWOE: Review and Recommendations", SWOE Program Office, US Army Cold Regions Research and Engineering Laboratory, Hanover, NH, SWOE Report 90-1, August.
2. Hummel, J.R., Jones, J.R., Longtin, D.R., and Paul, N.L. (1991) "Development of the Smart Weapons Operability Enhancement Interim Thermal Model", Phillips Laboratory, Hanscom AFB, Massachusetts, PL-TR-91-2073, March, ADA 238995.
3. Hummel, J.R., Jones, J.R., Longtin, D.R., and Paul, N.L. (1991) "Development of a 3-D Tree Thermal Response Model for Energy Budget and Scene Simulation Studies", Phillips Laboratory, Hanscom AFB, Massachusetts, PL-TR-91-2109, March, ADA 240509.
4. Balick, L.K., Link, L.E., Scoggins, R.K., and Soloman, J.L. (1981) "Thermal Modeling of Terrain Surface Elements," U.S. Army Engineer Waterways Experiment Station, EL-81-2, March, ADA 098019.
5. Marshall, T.J. and Holmes, J.W., (1988) *Soil Physics*, Second edition, Cambridge University Press, Cambridge.
6. Lienhard, J.H. (1981) *A Heat Transfer Textbook*, Prentice-Hall Inc., New Jersey.
7. Carslaw, H. S. and Jaeger, J. C. (1959) *Conduction of Heat in Solids*, Second Edition, Oxford University Press, Glasgow.
8. Hummel, J.R., Paul, N.L., Jones, J.R., Longtin, D.R. (1991) "STAMP - The SWOE Thermal Analysis and Measurement Program: Summary of the 1990 Field Tests." Phillips Laboratory, Hanscom AFB, Massachusetts, PL-TR-91-2242, 8 October.

Appendix A

Summary of SPARTA'S TRAC-3 3-D Thermal Response Code

A.1 Introduction

TRAC-3 is a general purpose, one, two, or three dimensional thermal analysis code. The code can be used for heat transfer studies on three dimensional surfaces with complicated geometries. These surfaces can include imbedded or protruding objects with different compositions and geometries.

TRAC-3 includes processes such as material removal due to decomposition and/or vaporization. Optional boundary conditions include surface or in-depth heating and re-radiation to the environment or other nodes.

The TRAC-3 program is designed for generalized heat transfer problems. In recent years, it has been extensively adapted by SPARTA personnel to simulate material response to laser radiation including thermal conduction and ablation (mass removal). The code is written in FORTRAN 77 and runs on SPARTA's SUN 4 computer. The code is not proprietary, but many of the adaptations for specific laser interactions have not been documented in a form suitable for general distribution.

A.2 Discussion

The TRAC-3 model is an extension of the Thermal Analysis of Satellite Components (TASC) model that was developed by SAIC for the Air Force Weapons Laboratory. TASC was developed to model the thermal analysis of satellite components in the space environment where radiative exchange and internal conduction determine the temperature. The TRAC-3 code has been extensively modified by SPARTA personnel over the years to include the addition of mass removal, transpiration, in-depth ablation, pyrolysis, and sophisticated representations of thermal states.

The model, in its present form, uses up to 2,500 fixed nodes and an implicit solution scheme. The use of fixed nodes enables the wide variety of different materials and geometries to be handled. A Crank-Nicolson method is used to set up the coefficients of the simultaneous equations and a modified Gauss-Seidel iterative approach is used to solve the equations.

The code can handle material properties that are either constant or temperature dependent. The axial conductivity can be treated differently from the radial conductivity. The code requires as input material densities, specific heats, conductivities, and absorptivities. For the assumed materials, one can either inhibit state changes or permit state changes to occur. The state changes permitted include melting, solidification, and/or vaporization. The code also handles non-reversible decomposition using temperature dependent rate equations. TRAC-3 allows for varying boundary conditions such as constant or time-varying heat flux; radiation to the

environment, other components, and/or a surface clearing flow, such as would occur in a laser material study; pyrolysis; or surface vaporization of materials. The convective cooling term provides a method for including natural convection losses that would be important for SWOE applications.

The model has the basic capability to handle transpiration in one dimension but it has not been implemented in past laser interaction studies since transpiration was known to be a small correction for those applications and because it would extend the run time. Transpiration would be important for the SWOE application.

TRAC-3 can include the pyrolysis of materials. The model allows for pyrolyzing materials to decompose by three independent rates and treats char formation as a separate process. It includes the possibility of in-depth vaporization in porous materials. Temperature and state-dependent conductivities can be specified in three independent directions. TRAC-3 is used whenever three dimensional heat transfer is important, whenever there are several different materials, and for detailed micromodeling of the thermal response of embedded materials, such as the thermal response of fibers and matrix in an hardening material.